Dual-Band Microstrip Antenna for the Fifth Generation Indoor / Outdoor Wireless Applications

Mourad S. Ibrahim

Department of Communications and Networks Engineering
Prince Sultan University, Riyadh, 11586, KSA
mrizk@psu.edu.sa
On Vacation: Modern Sciences and Arts University, 6th October City. Egypt.

Abstract ─ In this paper a dual band monopole antenna with omnidirectional radiation pattern suitable for indoor and outdoor fifth generation (5G) applications at 28 GHz and 60 GHz systems is developed. The proposed monopole antenna is built up using a microstrip of two rectangular patches and a T-shaped folded patch. The analysis and optimization processes throughout this paper are carried out using a High Frequency Surface Structure (HFSS) that uses the Finite Element Method (FEM) numerical method, and CST Microwave Studio that uses the Finite Integral Technique (FIT) numerical method. Good agreement between the two methods is obtained. The bandwidth of the lower and upper bands is about 1.44 GHz (5.1%) and 39.24 GHz (60.6%), respectively. The antenna directivity is about 2.28 dBi at 28GHz with a total efficiency of 93% and about 3.414 dBi with a total efficiency of 97.5% at 60GHz.

Index Terms ─ Dual band, Fifth generation, LMDS, Omnidirectional pattern, WiGig.

I. INTRODUCTION

The exponential growth of telecommunication over the past three decades increases the amount of data the average person uses exponentially. This growth is more noteworthy especially with the evolution of wireless communications which requires the development of low cost, lightweight, and low profile antennas that are capable of maintaining high performance over a wide bandwidth [1].

The global bandwidth shortage facing wireless carriers has motivated the exploration of the underutilized millimeter wave (mm-wave) frequency spectrum for future broadband communication networks [2].

Due to the importance of multiband single feed patch antennas in enormous millimeter wave applications, various techniques can be found in literature for multiband planar antenna designs as in [3-16]. For example, multiband microstrip antennas operating at around 35 GHz using semi-insulating multilayer GaAs is described in [3]. In [4], dual band 24/60 GHz with bandwidth not exceed 1.2% and gain of -9 dB at the lower band and of 1 dB at the upper band is presented. A meta-resonator antenna in [5] with two operating frequencies (41 & 52.2) GHz using a pair of SRRs with 2% bandwidth, 3.76 dB gain, and 71% efficiency is proposed. In [6], two modes are excited to achieve a dual band (58 & 77) GHz with -2 dB and 0.3 dB gain respectively and nearly 6% bandwidth at both frequencies. A novel hybrid configuration, using coplanar patches and a slot in feed line, has been proposed in [8] to achieve dual band response at 83 and 94 GHz.

In this paper, the design and the simulation of a dual band microstrip planar antenna are presented. The proposed antenna is operating at the 28 GHz (Ka - band) for LMDS which currently considered for 5G mobile cellular [17], and the 60 GHz (V - band) for Wireless Gigabit Alliance (WiGig) applications [18].

II. ANTENNA STRUCTURE AND DESIGN

Fig. 1 shows the proposed monopole antenna structure geometry in perspective and top view. As noted, the antenna patch consists of a T-folded shape with two rectangular patches with partial ground plane [19]. The patch mounted on substrate FR4 with a relative dielectric constant of 4.4. The dimensions of the antenna structure are shown in Fig. 2. The substrate dimension is W_s by L_s while the partial ground is W_s by L_g. The T-folded shape has dimensions W_t by L_t for the mid and L_{top} for top and L_{fold} for folded side. The two rectangular patches have dimensions W_p by L_p.

The microstrip transmission line feeder dimesion is W_f by L_f. The characteristic parameters of the microstrip can be found by using the following expressions [20]:

When $\frac{w}{h} \le 1$, the characteristic

$$Z_c = \frac{60}{\sqrt{\varepsilon_{reff}}} \ln\left[\frac{8h}{w} + \frac{w}{4h}\right] \quad (1)$$

Where

$$\varepsilon_{reff} = \frac{\varepsilon_r + 1}{2} + \frac{\varepsilon_r - 1}{2} \times \left\{\left[1 + 12\frac{h}{w}\right]^{-1/2} + 0.04\left[1 - \frac{w}{h}\right]^2\right\} \quad (2)$$

While when $\frac{w}{h} > 1$

$$Z_c = \frac{\frac{120\pi}{\sqrt{\varepsilon_{reff}}}}{\frac{w}{h} + 1.393 + 0.667 \ln\left[\frac{w}{h} + 1.444\right]} \quad (3)$$

Where

$$\varepsilon_{reff} = \frac{\varepsilon_r + 1}{2} + \frac{\varepsilon_r - 1}{2}\left[1 + 12\frac{h}{w}\right]^{-1/2} \quad (4)$$

In the expressions, h represents the substrate height, w represents the transmission line width, and ε_{reff} represents the effective dielectric constant.

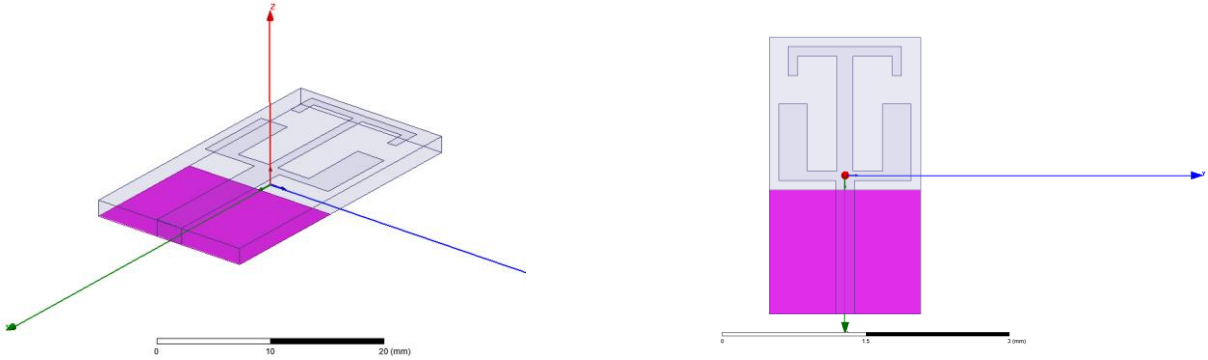

(a) (b)

Fig.1. Geometry of the proposed dual band antenna a) Perspective view b) Top view.

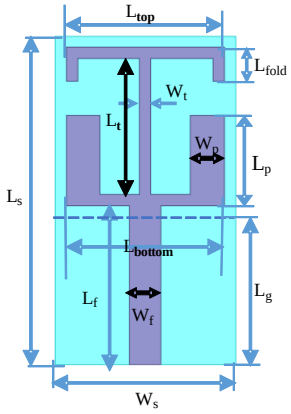

Fig.2. Antenna structure with dimensions.

III. PARAMETRIC STUDY

The effect of varying antenna dimensions L_{fold}, L_{top}, L_{bottom}, L_P, W_P, and L_t are shown in figures 3 to 8. The dimensions of the substrate, ground, and feeder are kept unchanged. With increasing L_{top} of the horizontal part of T-shaped, the lower resonant frequency is decreased with unchanged bandwidth whereas the upper bandwidth is decreased as shown in Fig. 3. Fig. 4 shows the effect of varying L_{bottom} on the return loss. As noted from the figure, by increasing the L_{bottom}, the lower resonant frequency almost is unchanged whereas the resonant frequency of the upper band is increased with a little increase in the bandwidth. With increasing the W_P, the upper and the lower resonant frequencies are almost unchanged as shown in Fig. 5. As the length of rectangular patch L_P increases, the upper and lower resonant frequency are decreased but the antenna matching becomes worse. Lower bandwidth increases whereas the upper bandwidth decreases as shown in Fig. 6. Fig. 7 illustrates the return loss varies with L_{fold}. As L_{fold} increases the lower resonant frequency decreases while upper resonant frequency remains unchanged whereas the lower bandwidth is not affected, the upper bandwidth is a little decreased as shown

in Fig. 7. With increasing L_t, the lower and the upper resonant frequencies are not affected whereas the upper bandwidth is decreased; the lower bandwidth is unchanged as shown in Fig. 8.

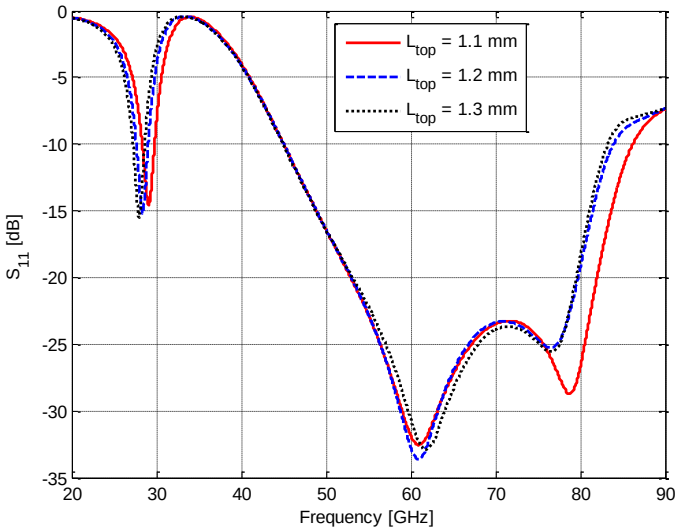

Fig. 3. Return loss of proposed antenna with varying L_{top}.

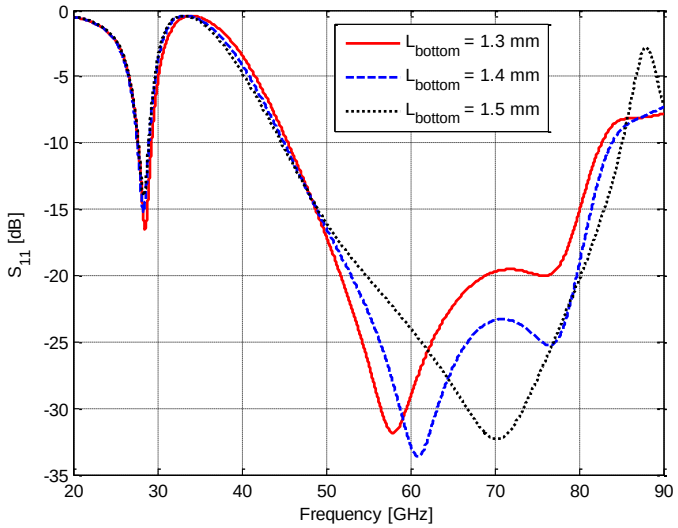

Fig. 4. Return loss of proposed antenna with varying L_{bottom}.

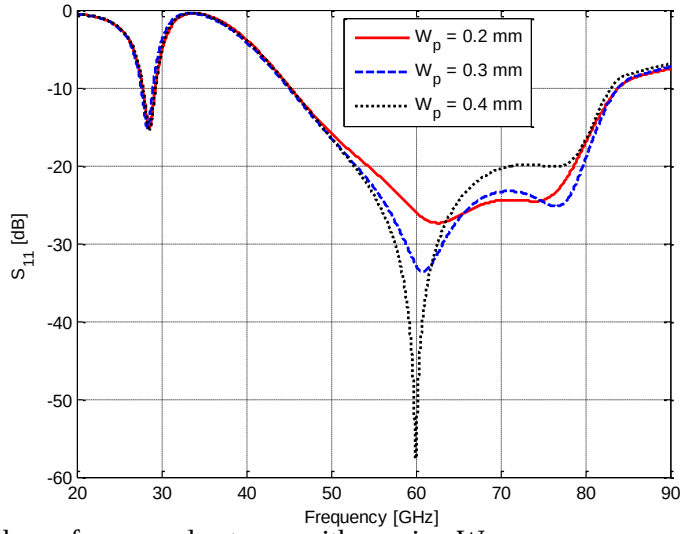

Fig. 5. Return loss of proposed antenna with varying W_p.

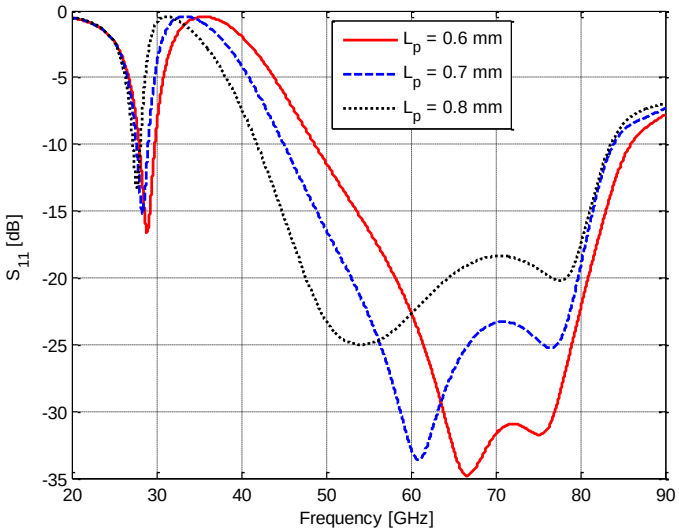

Fig. 6. Return loss of proposed antenna with varying L_p.

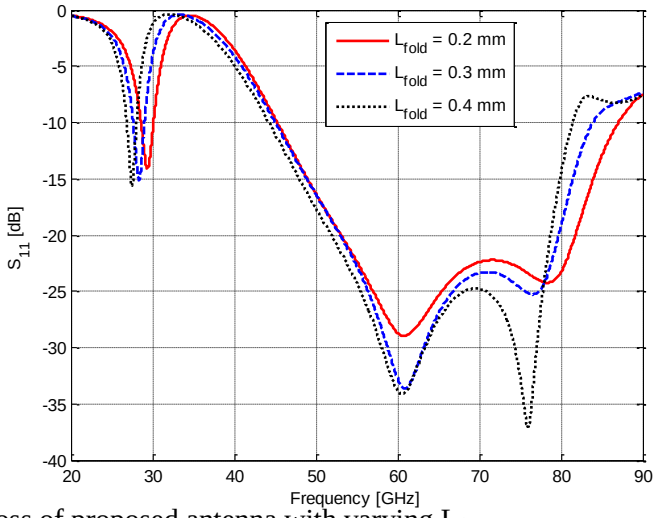

Fig. 7. Return loss of proposed antenna with varying L_{fold}.

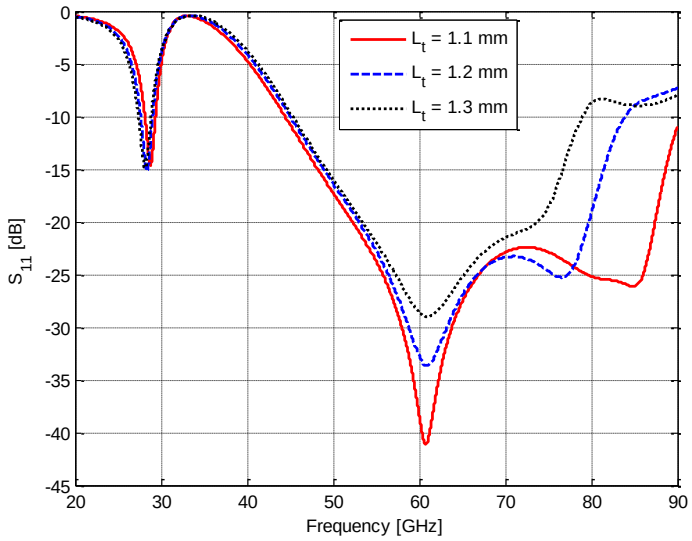

Fig. 8. Return loss of proposed antenna with varying L_t.

IV. ANTENNA SIMULATION RESULTS

In order to get optimized design dimensions a parametric analysis is carried out to achieve dual band antenna at 28 GHz and 60 GHz with acceptable performance. The optimized design dimensions are illustrated in Table 1.

In order to verify our results, the proposed antenna is simulated using two different methods, FIT (commercial software CST) and FEM (commercial software HFSS). Fig. 9 shows the reflection coefficient for the proposed antenna using FIT, and FEM. Matching is better in FEM and there is a small deviation in the upper band between the two methods. It's noted in Fig. 9 that, the antenna achieve good impedance matching over the dual band and the impedance bandwidth for $S_{11} \leq$ -10 dB in lower band is from 27.52 to 28.96 GHz which covers the LMDS frequency band while in upper band is from 45.14 to 84.38 GHz which covers the WiGig frequency band.

The center frequency of the lower band is 28.24 GHz with bandwidth 5.1 % while the center frequency for the upper band is 64.76 GHz with bandwidth 60.6%. The VSWR using FIT and FEM is illustrated in Fig. 10 with VSWR ≤ 2 in the antenna upper and lower bandwidths.

The antenna real and imaginary input impedance for the proposed antenna is illustrated in Fig. 11. It's noted from Fig. 11 that, the real part of the input impedance is approximately 50 Ω at the antenna bandwidth while the reactance part tends to zero.

Table 1: Optimized dimensions of the proposed antenna in mm.

Parameter	Value	Parameter	Value
W_s	1.6	W_p	0.3
L_s	2.9	L_p	0.7
L_g	1.3	W_t	0.1
W_f	0.2	L_t	1.2
L_f	1.4	L_{top}	1.2
L_{fold}	0.3	L_{bottom}	1.4

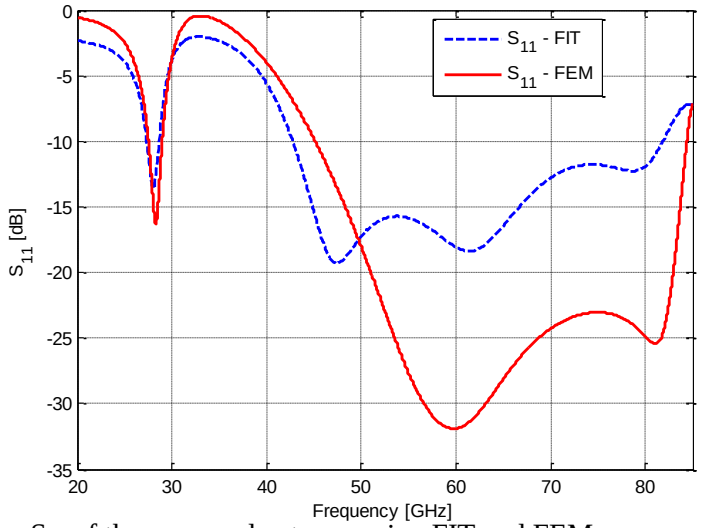

Fig. 9. Return loss S_{11} of the proposed antenna using FIT and FEM.

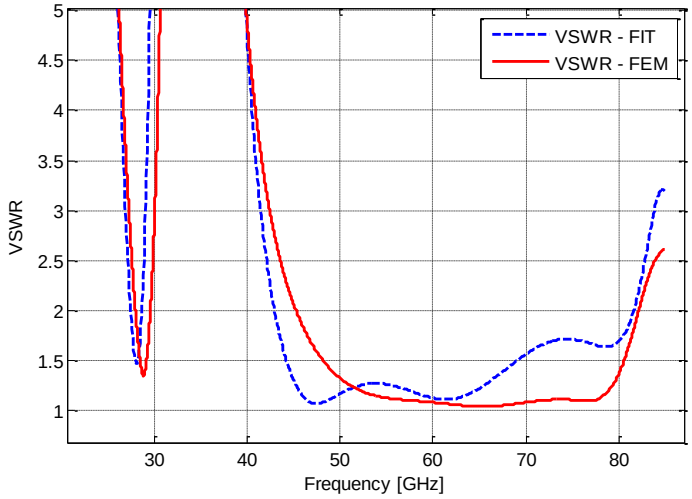

Fig. 10. VSWR of proposed antenna using FIT and FEM.

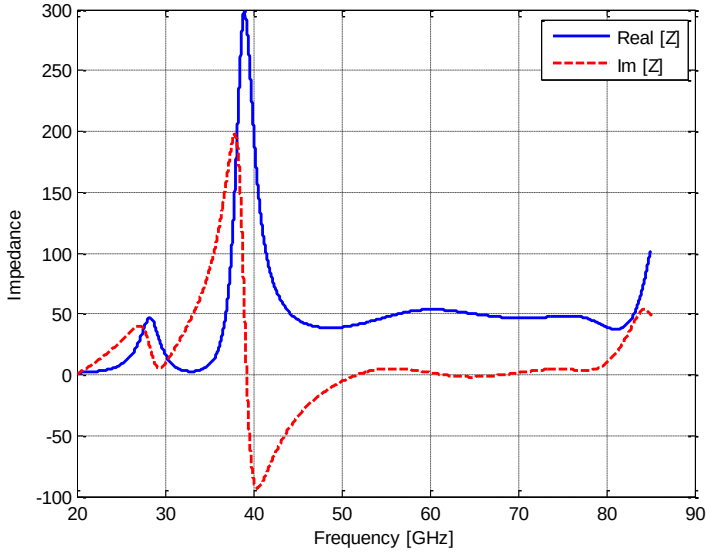

Fig. 11. The real and imaginary part of input impedance for the proposed antenna.

Fig. 12 shows the omnidirectional pattern at 28 and 60 GHz. Fig. 12 (a) shows the directivity pattern at 28 GHz with maximum directivity of 2.28 dBi and the total efficiency is 93 %. While Fig. 12 (b) shows the directivity pattern at 60 GHz with maximum directivity of 3.414 dBi and the total efficiency is 97.5%.

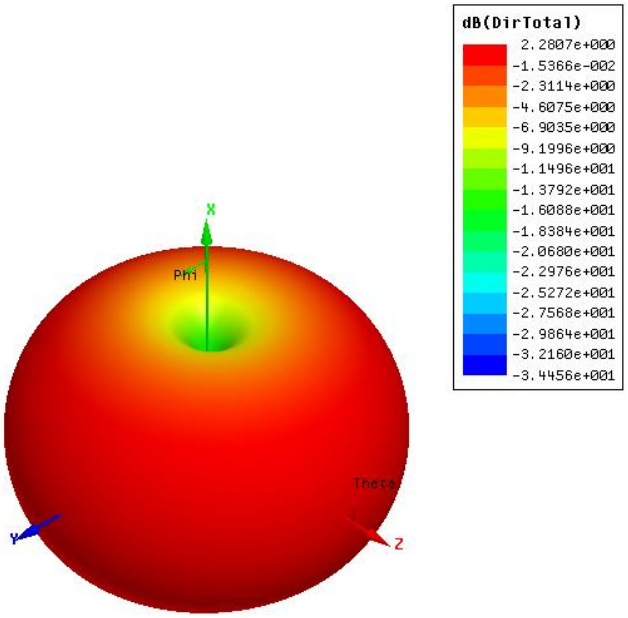

(a)

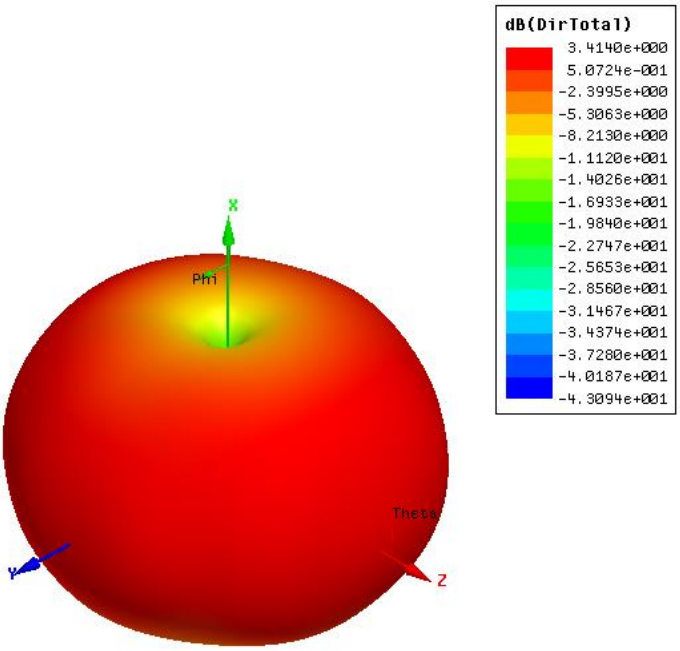

(b)

Fig 12. Simulated directivity patterns at a) 28 GHz with maximum directivity 2.28 dBi and at b) 60 GHz with maximum directivity 3.414 dBi.

V. CONCLUSION

In this paper, a monopole microstrip antenna with partial ground plane is designed and simulated. The lower band centered at 28.24 GHz with bandwidth of 1.44 GHz (5.1%). The upper band centered at 64.76 GHz with broad bandwidth suitable for WiGig of about 39.24 GHz (60.6%). The antenna radiation pattern is omnidirectional with maximum directivity of 2.28dBi and 3.414 dBi at 28 GHz and 60 GHz respectively. The total efficiency at 28 GHz and 60 GHz exceeds 93%. The simulation is carried out using FIT and FEM and good agreement between the two methods is obtained.

REFERENCES

[1] S. S. Jaco du Preez, *Millimeter-Wave Antennas: Configurations and Applications*: Springer International Publishing Switzerland, 2016.

[2] T. S. Rappaport, S. Sun, R. Mayzus, H. Zhao, Y. Azar, K. Wang, G. N. Wong, J. K. Schulz, M. Samimi, and F. Gutierrez, "Millimeter wave mobile communications for 5G cellular: It Will Work!," *IEEE Access*, vol. 1, pp. 335-349, 2013.

[3] D. Sanchez-Hernandez, Q. H. Wang, A. A. Rezazadeh, and I. D. Robertson, "Millimeter-wave dual-band microstrip patch antennas using multilayer GaAs technology," *IEEE Transactions on Microwave Theory and Techniques*, vol. 44, pp. 1590-1593, 1996.

[4] H. Jie-Huang, W. Jin-Wei, C. Yi-Lin, and C. F. Jou, "A 24/60GHz dual-band millimeter-wave on-chip monopole antenna fabricated with a 0.13-μm CMOS technology," in *2009 IEEE International Workshop on Antenna Technology*, pp. 1-4, 2009.

[5] I. K. Kim and V. V. Varadan, "Electrically small, millimeter wave dual band meta-resonator antennas," *IEEE Transactions on Antennas and Propagation*, vol. 58, pp. 3458-3463, 2010.

[6] T. Y. Lin, T. Chiu, and D. C. Chang, "Design of dual-band millimeter-wave antenna-in-package using flip-chip Aassembly," *IEEE Transactions on Components, Packaging and Manufacturing Technology*, vol. 4, pp. 385-391, 2014.

[7] D. Lee and C. Nguyen, "A millimeter-wave dual-band dual-polarization antenna on liquid crystal polymer," in *2014 IEEE Antennas and Propagation Society International Symposium (APSURSI)*, pp. 775-776, 2014.

[8] S. Agarwal, N. P. Pathak, and D. Singh, "Concurrent 83GHz/94 GHz parasitically coupled defected microstrip feedline antenna for millimeter wave applications," in *2013 IEEE Applied Electromagnetics Conference (AEMC)*, pp. 1-2, 2013.

[9] N. Ashraf, O. Haraz, M. A. Ashraf, and S. Alshebeili, "28/38-GHz dual-band millimeter wave SIW array antenna with EBG structures for 5G applications," in *2015 International Conference on Information and Communication Technology Research (ICTRC)*, pp. 5-8, 2015.

[10] G. N. Tan, X. X. Yang, and B. Han, "A dual-polarized Fabry-Perot cavity antenna at millimeter wave band with high gain," in *2015 IEEE 4th Asia-Pacific Conference on Antennas and Propagation (APCAP)*, pp. 621-622, 2015.

[11] H. Aliakbari, A. Abdipour, R. Mirzavand, A. Costanzo, and P. Mousavi, "A single feed dual-band circularly polarized millimeter-wave antenna for 5G communication," in *2016 10th European Conference on Antennas and Propagation (EuCAP)*, pp. 1-5, 2016.

[12] S. S. Siddiq, G. S. Karthikeya, T. Tanjavur, and N. Agnihotri, "Microstrip dual band millimeter-wave antenna array for UAV applications," in *2016 21st International Conference on Microwave, Radar and Wireless Communications (MIKON)*, pp. 1-4, 2016.

[13] Z. Wenyao, V. Miraftab, M. Repeta, D. Wessel, and T. Wen, "Dual-band millimeter-wave interleaved antenna array exploiting low-cost PCB technology for high speed 5G communication," in *2016 IEEE MTT-S International Microwave Symposium (IMS)*, pp. 1-4, 2016.

[14] M. M. M. Ali and A. R. Sebak, "Design of compact millimeter wave massive MIMO dual-band (28/38 GHz) antenna array for future 5G communication systems," in *2016 17th International Symposium on Antenna Technology and Applied Electromagnetics (ANTEM)*, pp. 1-2, 2016.
[15] Y. A. M. K. Hashem, O. M. Haraz, and E. D. M. El-Sayed, "6-Element 28/38 GHz dual-band MIMO PIFA for future 5G cellular systems," in *2016 IEEE International Symposium on Antennas and Propagation (APSURSI)*, pp. 393-394, 2016.
[16] S. Hwangbo, Y. K. Yoon, and A. Shorey, "Glass interposer integrated dual-band millimeter wave TGV antenna for inter-/intra chip and board communications," in *2016 IEEE International Symposium on Antennas and Propagation (APSURSI)*, pp. 1639-1640, 2016.
[17] S. Hur, S. Baek, B. Kim, Y. Chang, A. F. Molisch, T. S. Rappaport, K. Haneda, and J. Park, "Proposal on Millimeter-Wave Channel Modeling for 5G Cellular System," *IEEE Journal of Selected Topics in Signal Processing*, vol. 10, pp. 454-469, 2016.
[18] C. J. Hansen, "WiGiG: Multi-gigabit wireless communications in the 60 GHz band," *IEEE Wireless Communications*, vol. 18, pp. 6-7, 2011.
[19] W. H. Yang J., Lv Z., Wang H., "Design of miniaturized dual-band microstrip antenna for WLAN application," *Sensors*, vol. 16, pp. 1-15, 2016.
[20] C. A. Balanis, *Advanced Engineering Electromagnetics*, Second Edition ed.: JohnWiley & Sons, New York, 2012.